Impact of Multiple Cyclic Loads on the Cyclic and Post-Cyclic Behavior of Fine-Grained Soils

Veronica Kiuna¹; Beena Ajmera, Ph.D., P.E., M.ASCE²; and Binod Tiwari, Ph.D., P.E., F.ASCE³

¹Doctoral Student, Dept. of Civil, Construction, and Environmental Engineering, Iowa State Univ., Ames, IA. Email: vgkiuna@iastate.edu

²Assistant Professor, Dept. of Civil, Construction, and Environmental Engineering, Iowa State Univ., Ames, IA. Email: bajmera@iastate.edu

³Professor and Associate Vice President of Research and Sponsored Projects, California State Univ., Fullerton, Fullerton, CA 92831. Email: btiwari@fullerton.edu

ABSTRACT

Fine-grained soils subjected to seismic loading often exhibit instability or failure of slopes, foundations, and embankments. To understand the behavior of clay soils under multiple earthquake loads, kaolinite samples were prepared and tested in the laboratory using a cyclic simple shear device. Each sample was subjected to two cyclic events separated by different degrees of reconsolidation periods to simulate different levels of excess pore water pressure dissipation. The results indicated that the degree to which excess pore water pressure generated during the first cyclic event was dissipated affected the cyclic resistance of the soil during the second cyclic event. The post-cyclic undrained shear strength was also found to be a function of the degree to which excess pore water pressure from the first cyclic load was allowed to dissipate prior to the application of the second cyclic load.

INTRODUCTION

Fine-grained soils subjected to cyclic loads may experience a reduction in shear strength due to increases in pore pressures. This reduction can have disastrous consequences for the geotechnical systems located on, within, or built using these materials (Ajmera et al. 2019, Boulanger and Idriss 2007). One example is the ground failure in the Lokanthali, Nepal, after the 2015 Gorkha earthquake. This failure was unexpected since the ground was at a gentle slope of about 4°. FLAC analyses by Tiwari et al. (2018) revealed that the additional stresses induced by the ground motions were insufficient to cause the widespread damage in the region. However, when strength degradations of the underlying black cotton soil (kalimati) were incorporated, the results better resembled the in-situ conditions of ground failure at Lokanthali after the earthquake (Tiwari and Pradel 2017, Tiwari et al. 2018). Some other examples include deep-seated slope failures observed after the 1964 Alaska, 1964 Niigata, 1978 Miyagi-ken Oki, and 1983 Sea of Japan earthquakes (Hyodo et al. 2000, Stark and Contreras 1998, Boulanger and Idriss 2004), damages to the Moss Landing Marine Facilities after 1989 Loma Prieta earthquake (Boulanger et al. 1998) and foundation failures after the 1999 Chi-Chi earthquake (Chu et al. 2008).

Previous work on the post-cyclic response has primarily focused on shear strength and deformation behavior of fine-grained soils after a single cyclic load. Several studies have reported the post-cyclic shear strength or the shear strength after cyclic loading. However, their primary focus has been on the influence of plasticity characteristics finding that soils with higher

plasticity indices experience a lower reduction in shear strength (Hyodo et al. 2000, Bray et al. 2004, Bray and Sancio 2006, Gratchev et al. 2006, Guo and Prakash 1999, Ishihara and Yasuda 1980, Prakash and Sandoval 1992, Tan and Vucetic 1989, Bahr 1991, Ishihara 1993, and Matsui et al. 1999). Several researchers (Thammathiwat and Chim-oye 2004, Azzouz et al. 1989, and Yasuhara 1994) derived relationships between reductions in shear strength and the increase in excess pore pressure due to cyclic loading. Others have examined the effects of pore pressure dissipation between cyclic loads on the post-cyclic shear strength (Yasuhara and Andersen 1989 and Teachavorasinsku et al. 2001).

Ajmera et al. (2017) subjected seventeen laboratory-prepared normally consolidated soil mixtures to sinusoidal loading at a frequency of 0.5 Hz using a cyclic simple shear device. They concluded that cyclic resistance increases with an increase in the plasticity index in soils with plasticity indices less than 60. However, the cyclic resistance will decrease with an increase in plasticity index in soils with plasticity indices greater than 60. Ajmera et al. (2019) used static and cyclic simple shear results from eighteen laboratory-prepared and nine natural soils to establish relationships that quantify the reductions in undrained shear strength resulting from a single cyclic load. However, earthquakes are rarely an isolated cyclic loading event. Rather the main shock of an earthquake is often preceded by a series of foreshocks and/or followed by a sequence of aftershocks. Although the multiple events surrounding a seismic event will affect the cyclic and post-cyclic behavior of soils, there is limited research on this topic. Thus, there is a need for continued research and a better understanding of the behavior of fine-grained soils under multiple cyclic loading events.

To address the gap in the understanding of the effects of multiple cyclic loads on the behavior of fine-grained soils, this study presents the results of a series of cyclic direct simple shear tests conducted on laboratory-prepared samples of kaolinite. Each sample was subjected to two cyclic loads. The cyclic loads were separated by a reconsolidation period in which pore pressures generated by the first cyclic load were allowed to dissipate to different degrees before the second load was applied. The results obtained were used to evaluate the cyclic and post-cyclic behavior of kaolinite.

MATERIALS AND METHODS

Dry powdered kaolinite purchased from Ward's Natural Science was used in all of the testing conducted in this study. The maximum particle size of this clay was 0.02 mm. Approximately 70% of the particles were smaller than 0.002 mm. This kaolinite has a liquid limit of 73, a plasticity index of 28, and a specific gravity of 2.72.

Samples were prepared by mixing dry kaolinite with de-ionized water at its liquid limit and then allowed to hydrate for at least 24 hours before testing commenced. The resulting slurry was poured into a latex membrane laterally confined by a stack of Teflon® rings. Samples were prepared to be 63.5 mm in diameter and 25.4 mm in height. Once prepared, the sample was allowed to consolidate at a vertical stress of 25 kPa until primary consolidation was complete. The completion of the primary consolidation was monitored by examining real-time logarithm of time versus displacement curves. Next, the vertical stress was doubled to 50 kPa and then 100 kPa. Each increment was applied until the completion of the primary consolidation was established.

After the consolidation phase was completed, the sample was subjected to the first cyclic load. Cyclic loads applied in this study had sinusoidal waveforms with frequencies of 0.5 Hz.

The amplitude of the cyclic load was determined from the desired cyclic stress ratio (CSR), which is the ratio of amplitude of the cyclic load to effective vertical consolidation pressure. The cyclic load was applied until either the double amplitude shear strain reached 10% or for a maximum of 500 cycles, whichever occurred first. This termination criteria are in accordance with the recommendations in Ajmera et al. (2017, 2019). Some of the excess pore pressures generated during the application of the first cyclic load were then allowed to dissipate. The time required to achieve the desired degree of excess pore pressure dissipation was calculated based on the coefficient of consolidation for the sample. This coefficient was determined from the consolidation data. A total vertical stress of 100 kPa was maintained on the sample during this period of reconsolidation.

Once the desired degree of excess pore pressure dissipation had been achieved, the sample was subjected to a second cyclic load. As before, this cyclic load was also sinusoidal in nature with a frequency of 0.5 Hz and an amplitude determined from a second *CSR*. The termination criteria were identical to those associated with the first cyclic load. Immediately after the application of the second cyclic load, the sample was sheared at a shearing rate of 5% per hour. The shearing phase was terminated when the peak shear strength was measured or when a maximum shear strain of 25% was reached. This shearing rate and termination criteria are in agreement with the recommendations in ASTM D6528.

All of the testing was conducted in a GeoComp cyclic direct simple shear device. This is a fully-automated computer-controlled apparatus that applies vertical loads from a micro-stepper motor and horizontal loads using a servo motor. Both the horizontal and vertical load cells have capacities of 10 kN. All LVDTs have 50 mm capacities.

RESULTS AND DISCUSSION

Typical Results. An example of the behavior observed in the samples during the consolidation process is illustrated in Figure 1. In particular, Figure 1 presents the cumulative vertical strain against the time in logarithmic scale. The primary consolidation under each applied vertical stress was typically completed within about three hours of the stress application. The compression index was calculated and compared with the values presented by Tiwari and Ajmera (2011). The compression indices were very similar indicating that the cyclic direct simple shear device used in this study was able to maintain at-rest conditions during the consolidation process. Similar results were observed in all of the samples tested in this study.

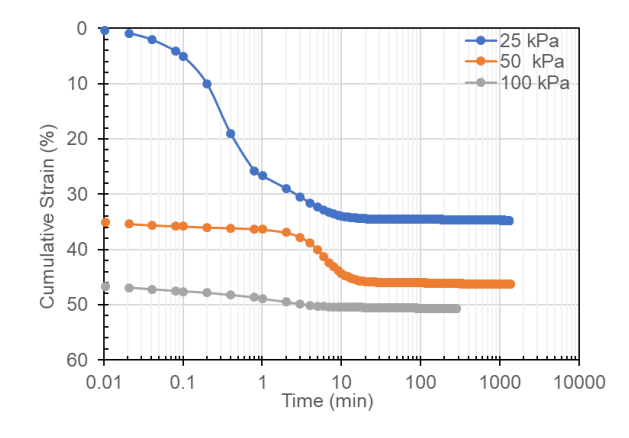


Figure 1. Logarithm of Time versus Cumulative Displacement for Kaolinite Tested.

Shown in Figure 2 are the typical responses of the kaolinite during the application of both cyclic loads. The sample in Figure 2 was subjected to cyclic stress ratio of 0.16 during the first cyclic load following which 100% of the excess pore pressure generated was allowed to dissipate before a second cyclic load with a cyclic stress ratio of 0.16 was applied. The solid lines in Figure 2 correspond the behavior observed during the application of the first cyclic load, while the dotted lines correspond to the second cyclic load. None of the samples generated sufficient excess pore pressures to liquefy. In other words, the effective stress was always greater than zero in all of the tests conducted.

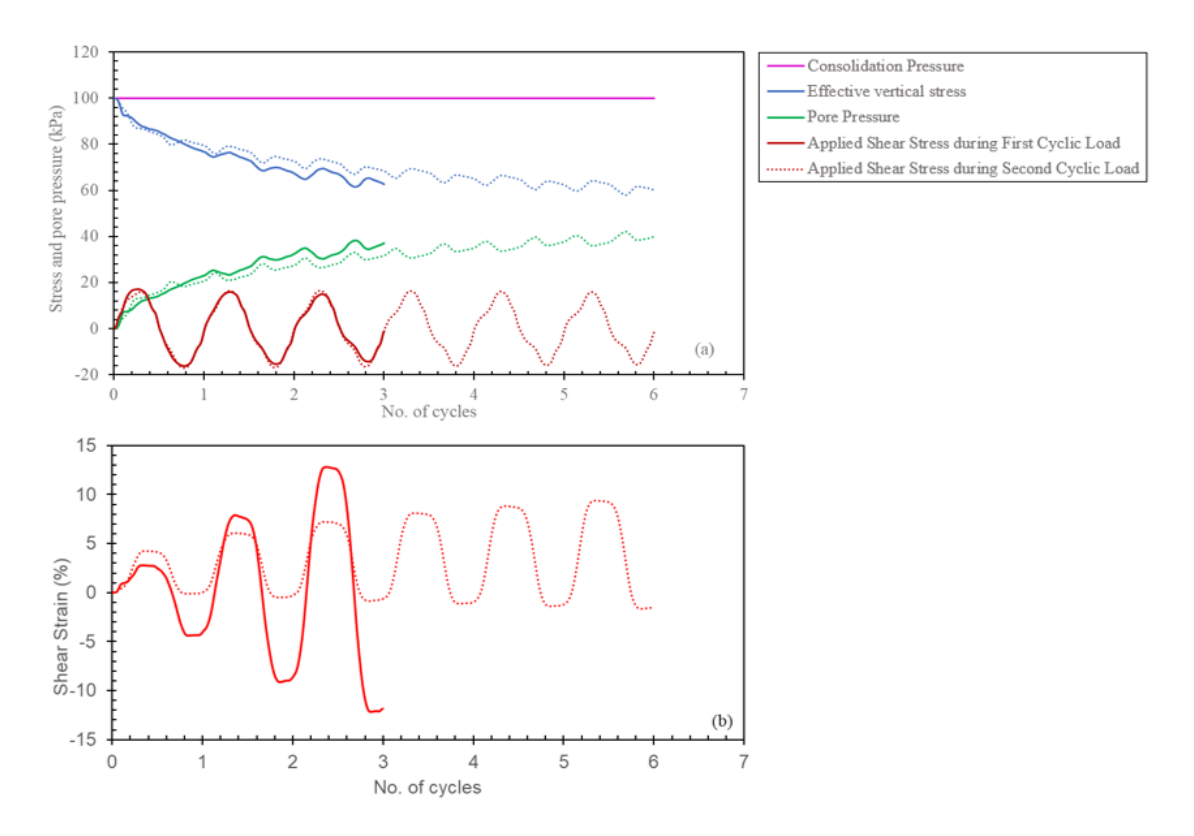


Figure 2. Typical Cyclic Response of the Kaolinite Samples Tested: (a) Stress and Pore Pressure and (b) Shear Strain. This figure corresponds to a sample first subjected to a cyclic load with *CSR*=0.16 with 100% pore pressure dissipation before the second cyclic load with *CSR*=0.16 was applied.

The number of cycles required to induce 10% double amplitude shear strain in the samples was always greater during the application of the second cyclic load in comparison to the first. This may be attributed to the densification of the sample that resulted from the dissipation of the excess pore pressures that resulted in a sample that is better able to resist the applied cyclic loads. Specifically, the vertical strain that occurred as the excess pore pressures were allowed to dissipate between the application of the two cyclic loads is summarized in Table 1. The results in Table 1 are for a kaolinite sample that was subjected to a cyclic load with a *CSR* of 0.16 with varying amounts of pore pressure dissipation before a second cyclic load with *CSR* of 0.16 was applied. Table 1 indicates that as the amount of excess pore pressure allowed to dissipate increased, the vertical strain that occurred in the sample also increased illustrating the densification that occurred within the sample.

Example stress-strain hystersis loops are provided in Figure 3. The results shown in this figure are from the same sample, whose response was depicted in Figure 2. In all of the samples tested, the hysteresis loops associated with the first cyclic load tended to be larger in area than those associated with the second cyclic load. This implies that the soil dissipated a greater amount of energy from the cyclic load during the first cyclic load. The higher density of the soil mass as a result of the dissipation of excess pore pressures between the application of cyclic loads may be the cause of this behavior (Table 1).

Table 1. Vertical Strain as a Function of Pore Pressure Dissipation. This table corresponds to kaolinite samples first subjected to a cyclic load with *CSR*=0.16 with varying amounts of pore pressure dissipation before the second cyclic load with *CSR*=0.16 was applied.

Degree of Pore Pressure Dissipation (%)	Vertical Strain Between Cyclic Loads (%)
20	1.26
40	1.62
60	1.88
80	2.38
100	2.92

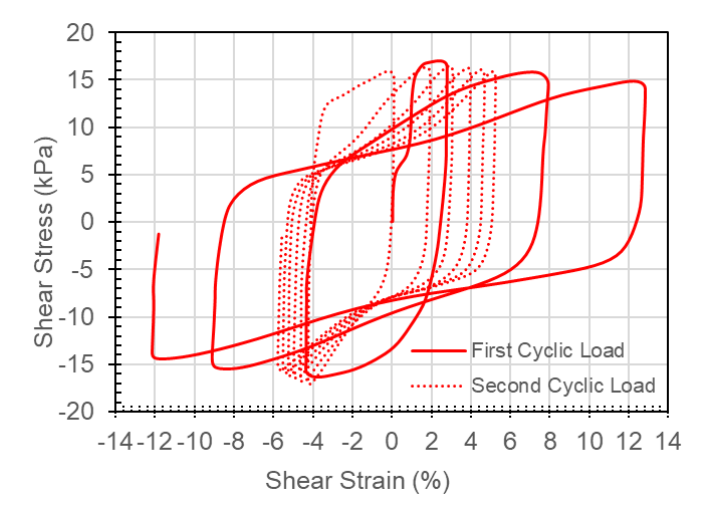


Figure 3: Example Stress-Strain Hysteresis Loops. This figure corresponds to a kaolinite sample that was first subjected to a cyclic load with *CSR*=0.16 with 100% pore pressure dissipation before second cyclic load with *CSR*=0.16 was applied.

Cyclic Strength Curves. Cyclic strength curves provide a visual representation of the cyclic resistance of a soil mass during a seismic event. Ajmera et al. (2017) presented cyclic strength curves for the samples they tested including the kaolinite used in this study. However, those results were only for samples subjected to a single cyclic load. Given that the behavior of the first cyclic load should be similar to that presented by Ajmera et al. (2017), this paper will focus on discussing the cyclic strength curves obtained during the application of the second cyclic load.

A typical cyclic strength curve for the kaolinite tested in this study is shown in Figure 4. The horizontal axis in Figure 4 corresponds to the number of cycles required to cause 2.5% double amplitude shear strain during the second cyclic load. The results at other double amplitude shear strains were similar. As expected, an increase in the severity of the cyclic load resulted in a decrease in the number of cycles required to induce 2.5% double amplitude shear strain.

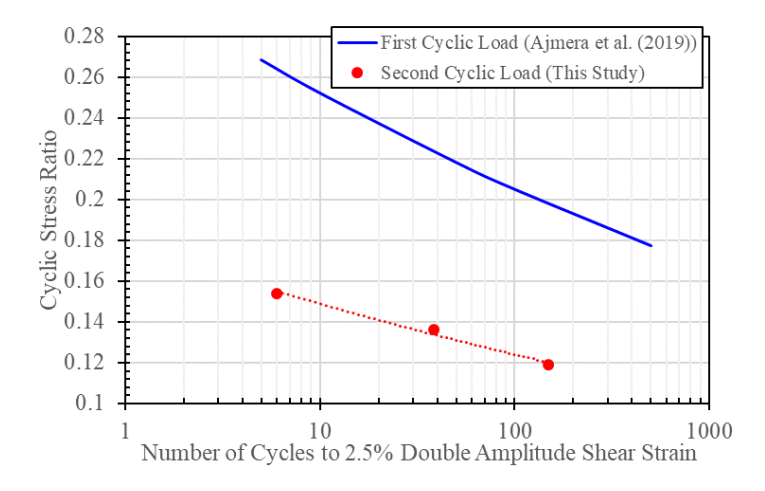


Figure 4. Typical Cyclic Strength Curves during Second Cyclic Load. Results in this figure correspond to a kaolinite sample subjected to a first cyclic load with *CSR*=0.16 followed by 80% dissipation of generated excess pore pressure.

Ajmera et al. (2017) and Ishihara et al. (1980) noted that cyclic strength curves can be represented with power functions, as in Equation 1. Here, N represents the number of cycles required to cause the desired double amplitude shear strain, while a and b are curve fitting parameters. Figure 5 shows variation of the power function parameters, a and b, with the degree of pore pressure dissipation.

$$CSR = aN^b \tag{1}$$

The value of the curve fitting parameter a is seen to increase with an increase in the degree of pore pressure dissipation (Figure 5a). Figure 5b shows that the value of curve fitting parameter b remains more or less constant with changes in the degree of pore pressure dissipation. This indicates that the cyclic strength curves will have a constant slope, but will shift upward as excess pore pressures generated during the first cyclic load are allowed to dissipate. In other words, as the soil mass densifies as a result of the dissipation of excess pore pressures, its cyclic resistance will increase. It is noted that the amount of pore pressure generated during the first cyclic load will have an effect on the power function parameters and the cyclic resistance during the application of the second cyclic load. However, in this figure, since all of the samples were prepared in a similar manner and subjected to the same first cyclic load, the excess pore pressures generated during the first cyclic load are similar. Thus, this effect of the amount of pore pressure generated during the first cyclic load is beyond the scope of this study.

Degradation Ratio. Ajmera et al. (2019) quantified the reduction in the undrained shear strength that results in fine-grained soils after the application of a single cyclic load. The undrained shear strength available after the application of the second cyclic load is expected to

be a function of the severity of the first cyclic load and the degree to which pore pressures generated during the first cyclic load are dissipated before a second cyclic load is applied. Figure 6 presents the variation in the degradation ratio with degree of pore pressure dissipation. The degradation ratio is defined as the ratio of the undrained shear strength of the sample measured immediately after the application of the second cyclic load to the static undrained shear strength of the sample. For the kaolinite tested in this study, the undrained strength ratio was 0.30. Figure 6 shows that as the degree of pore pressure dissipation increases, the degradation ratio increases. This indicates that as more of the pore pressure generated after the application of the first cyclic load is allowed to dissipate, lower reductions in the undrained shear strength as a result of the second cyclic load are observed.

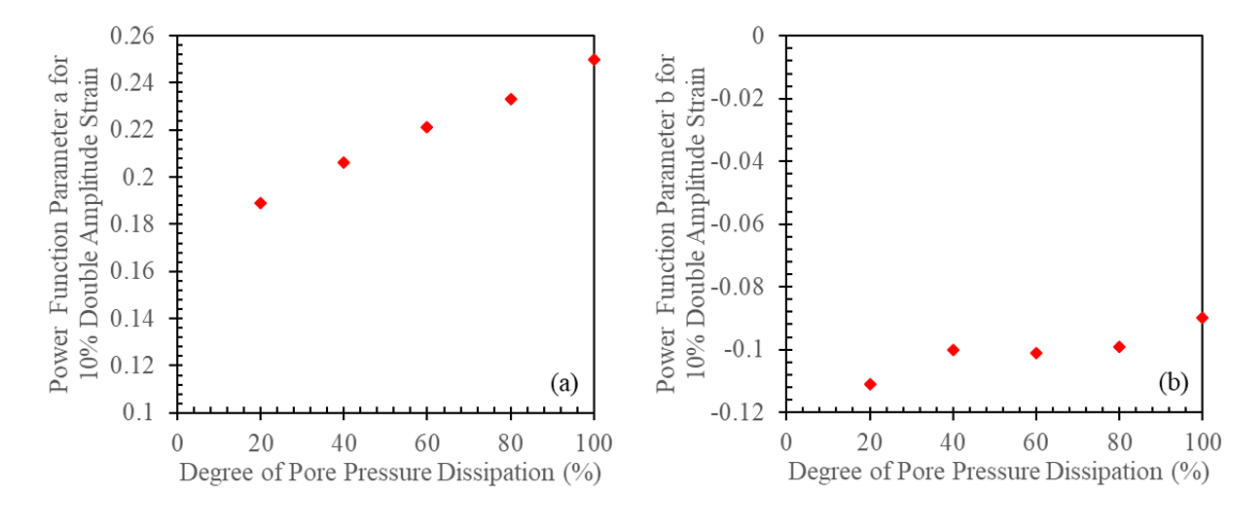


Figure 5. Influence of the Degree of Pore Pressure Dissipation on Power Function Parameter (a) *a* and (b) *b*. Results presented correspond to samples subjected to a first cyclic load with *CSR*=0.16.

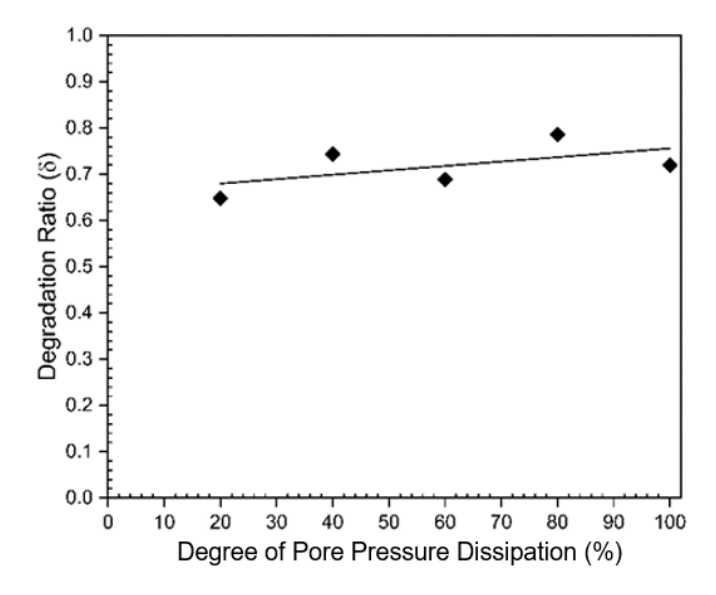


Figure 6. Effect of Pore Pressure Dissipation on the Degradation Ratio.

CONCLUSIONS

Seismicity in the field will typically consist of several cyclic loads in the form of foreshocks, the main shock and the aftershock. Thus, there is a need to understand how multiple cyclic loads will impact the behavior of fine-grained soils during and after the cyclic loads. To capture this behavior, this study performed cyclic simple shear tests on kaolinite subjected to two cyclic loads separated between which various degrees of excess pore pressure dissipation was permitted. Both the cyclic resistance during the application of the second cyclic load as well as the undrained shear strength immediately after the second cyclic load were impacted by the length of the reconsolidation period. Specifically, as excess pore pressures generated during the first cyclic load were allowed to dissipate, the cyclic resistance of the kaolinite increased. Similarly, the degradation ratio also increased with an increase in the degree to which excess pore pressures were allowed to dissipate. Both of these may be attributed to the densification of the soil mass which inherently occurred as the excess pore pressures dissipated.

ACKNOWLEDGEMENTS

This material is based upon work supported by the National Science Foundation under Grant No. 2224135. The authors would also like to acknowledge the financial support provided by the College of Engineering and the Department of Civil, Construction and Environmental Engineering at both Iowa State University and North Dakota State University, and the North Dakota ESPCOR STEM grants program. Mr. Muhammad Shahid Iqbal is thanked for performing some of the cyclic simple shear tests for this study.

REFERENCES

- Ajmera, B., Brandon, T., and Tiwari, B. (2017). "Influence of Index Properties on Shape of Cyclic Strength Curves for Clay-Silt Mixtures." *Soil Dynamics and Earthquake Engineering*, 102, 46-55.
- Ajmera, B., Brandon, T., and Tiwari, B. (2019). "Characterization of the Reduction in Undrained Shear Strength in Fine-Grained Soils due to Cyclic Loading." *Journal of Geotechnical and Geoenvironmental Engineering*, 145(5), 04019017.
- ASTM. ASTM D6528. (2007). Standard Test Method for Consolidated Undrained Simple Shear Testing of Cohesive Soils. American Society of Testing and Materials.
- Azzouz, A. S., Malek, A. M., and Baligh, M. M. (1989). "Cyclic Behavior of Clays in Undrained Simple Shear." *Journal of Geotechnical Engineering*, 115(5), 637–657.
- Bahr, M. A. (1991). *Mechanical Behavior and Modeling of Saturated Clays Subjected to Cyclic Loading*. PhD Thesis, Osaka University.
- Boulanger, R. W., and Idriss, I. M. (2007). "Evaluation of Cyclic Softening in Silts and Clays." *Journal of Geotechnical and Geoenvironmental Engineering*, 133(6), 641-652.
- Boulanger, R. W., and Idriss, I. M. (2004). "Evaluating the Potential for Liquefaction or Cyclic Failure of Silts and Clays." Report No. UCD/CGM-04/01, University of California, Davis.
- Boulanger, R., Meyers, M. W., Mejia, L. H., and Idriss, I. M. (1998). "Behavior of a Fine-Grained Soil during the Loma Prieta Earthquake." *Canadian Geotechnical Journal*, 35(1), 146–158.

- Bray, J. D., and Sancio, R. B. (2006). "Assessment of the Liquefaction Susceptibility of Fine-Grained Soils." *Journal of Geotechnical and Geoenvrionmental Engineering*, 132(9), 1165–1177.
- Bray, J. D., Sancio, R. B., Riemer, M. and Turan Durgunoghr, H. (2004). "Liquefaction Susceptibility of Fine-grained Soils." *Proceedings of the 11th International Conference on Soil Dynamics and Earthquake Engineering and 3rd International Conference on Earthquake Geotechnical Engineering*, 655-662.
- Chu, D. B., Stewart, J. P., Boulanger, R. W., and Lin, P. S. (2008). "Cyclic Softening of Low-Plasticity Clay and Its Effect on Seismic Foundation Performance." *Journal of Geotechnical and Geoenvironmental Engineering*, 134(11), 1595–1608.
- Gratchev, I. B., Sassa, K., Osipov, V. I., and Sokolov, V. N. (2006). "The Liquefaction of Clayey Soils under Cyclic Loading." *Engineering Geology*, 86(1), 70–84.
- Guo, T., and Prakash, S. (1999). "Liquefaction of Silts and Silt-Clay Mixtures." *Journal of Geotechnical and Geoenvironmental Engineering*, 125(8), 706–710.
- Hyodo, M., Ito, S., Yamamoto, Y., and Fujii, T. (2000). "Cyclic Shear Behaviour of Marine Clays." *Proceedings of the 8th International Offshore and Polar Engineering Conference*, 557-563.
- Ishihara, K., and Yasuda, S. (1980). "Cyclic Strengths of Undisturbed Cohesive Soils of Western Tokyo." *Proceedings of the International Symposium on Soils under Cyclic and Transient Loading*, 57-66.
- Ishihara, K. (1993). "Liquefaction and Flow Failure during Earthquakes." *Géotechnique*, 43(3), 351–451.
- Ishihara, K., Troncoso, J., Kawase, Y., and Takahashi, Y. (1980). "Cyclic Strength Characteristics of Tailings Materials." *Soils and Foundations*, 20(4), 127–142.
- Matsui, T., Nabeshima, Y., and El Mesmary, M. A. (1999). "Degradation in Cyclic Shear Behavior And Soil Properties of Saturated Clays." *Proceedings of the 9th International Offshore and Polar Engineering*, 536-541.
- Prakash, S., and Sandoval, J. A. (1992). "Liquefaction of Low Plasticity Silts." *Soil Dynamics and Earthquake Engineering*, 11(7), 373-379.
- Stark, T. D., and Contreras, I. A. (1998). "Fourth Avenue Landslide during 1964 Alaskan Earthquake." *Journal of Geotechnical and Geoenviromental Engineering*, 124(2), 99–109.
- Tan, K., and Vucetic, M. (1989). "Behavior of Medium and Low Plasticity Clays under Cyclic Simple Shear Conditions." *Proceedings of the 4th International Conference on Soil Dynamics Engineering*, 401-409.
- Teachavorasinskun, S., Thongchim, P., and Lukkunaprasit, P. (2001). "Shear Modulus and Damping Ratio of a Clay during Undrained Cyclic Loading." *Géotechnique*, 51(5), 467–470.
- Thammathiwat, A., and Chim-oye, W. (2004). "Behavior of Strength and Pore Pressure of Soft Bangkok Clay under Cyclic Loading." *Thammasat International Journal of Science and Technology*, 9(4), 21-28.
- Tiwari, B., and Ajmera, B. (2011). "A New Correlation Relating the Shear Strength of Reconstituted Soil to the Proportions of Clay Minerals and Plasticity Characteristics." *Applied Clay Science*, 53(1), 48–57.
- Tiwari, B., and Pradel, D. (2017). "Ground Deformation at Lokanthali, Kathmandu due to the Mw 7.8 2015 Gorkha Earthquake." *Proceedings of Geotechnical Frontiers 2017 Geotechnical Special Publication*, 278, 333–342.

- Tiwari, B., Pradel, D., Ajmera, B., Yamashiro, B., and Khadka, D. (2018). "Landslide Movement at Lokanthali during the 2015 Earthquake in Gorkha, Nepal." *Journal of Geotechnical and Geoenvironmental Engineering*, 144(3), 05018001.
- Yasuhara, K. (1994). "Postcyclic Undrained Strength for Cohesive Soils." *Journal of Geotechnical Engineering*, 120(11), 1961–1979.
- Yasuhara, K., and Andersen, K. (1989). "Effect of Cyclic Loading on Recompression of Overconsolidated Clay." Congrès international de mécanique des sols et des travaux de fondations, 12, 485–488.